Supporting Information

Consecutive Dephosphorylation by Alkaline Phosphatase Directed in-Situ Formation of Porous Hydrogels of SF with Nanocrystalline Calcium Phosphate Ceramics for Bone Regeneration

Hang Li,[a] Jikun Zhang,[a] Shengnan Liu,[a] Yufei Yan,[*b,c] and Xinming Li[*a]

[a] College of Chemistry, Chemical Engineering and Materials Science, Soochow University, Suzhou, 215123, China.

[b] Department of Orthopaedic Surgery, Shanghai Jiao Tong University Affiliated Sixth People's Hospital, Shanghai, 200233, China.

[c] Shanghai Institute of Traumatology and Orthopaedics, Shanghai Key Laboratory for Prevention and Treatment of Bone and Joint Diseases, Ruijin Hospital, Shanghai Jiao Tong University School of Medicine, 197 Ruijin 2nd Road, Shanghai, 200025, PR China.

Email: xinmingli@suda.edu.cn; yanyufei2040@outlook.com

Contents

1. Materials and methods

Bombyx. mori cocoons were obtained from Nantong Xinsilu sericulture co. LTD (Jiangsu, China). 2-chlorotrityl chloride resin, Fmoc-L-Tyr(H_2PO_3)-OH, Fmoc-L-Phe-OH and Fmoc-Gly-OH were purchased from Shanghai GL Biochem (Shanghai, China). 2-(naphthalen-6-yl) acetic acid was provided by Aladdin (Shanghai, China). Alkaline phosphatase was obtained from Thermo Fisher Scientific. Calcium chloride was purchased from Sinopharm chemical reagent co. LTD (Shanghai, China). β-glycerophosphate disodium salt hydrate and hydroxyapatite were obtained from Sigma. Dulbecco's Modified Eagle Medium (DMEM), phosphate buffer saline (PBS), Fetal bovine serum (FBS) and penicillin-streptomycin (PS) were provided by Gibco (USA). 4% paraformaldehyde, staining dyes for live/dead and CCK8 assays were purchased from Dojindo Laboratories (Japan). All the other raw materials were purchased from Sigma and Enox Chemicals and used without further purification. ^{1}H and ^{31}P NMR spectra were obtained from an INOVA 400 MHz (USA) by using DMSO-d_6 as a solvent. MALDI-TOF MS analysis was conducted on a Bruker Ultraflex-Treme mass spectrometer (Germany). Circular dichroism spectra (CD) were collected from a JASCO J-810 spectrometer (Japan). Fourier transform infrared spectroscopy (FTIR) characterizations were performed on a Thermo Scientific Nicolet 6700 spectrophotometer (USA). Rheological tests were conducted on a Thermo Scientific HAAKE RheoStress 6000 rheometer (Germany). Scanning electron micrograph (SEM) images and Energy dispersive spectrometer (EDS) characterizations were recorded on a Hitachi S-4700 microscope (Japan). X-ray diffraction (XRD) characterizations were performed on an X'Pert-Pro MPD diffractometer (Netherlands). X-ray photoelectron spectroscopy (XPS) characterizations were carried out on a Thermo Fisher Scientific Escalab 250Xi spectrometer (USA). Fluorescence microscopy images were taken on a confocal laser scanning microscope (Zeiss, Germany). The bone micro-CT images were taken on a Scanco Medical micro-CT system (Switzerland).

2. Experimental section

2.1 Preparation of SF solution. Cocoons of *Bombyx mori* was boiled in an aqueous solution of 0.02 M Na_2CO_3 for 1 h, followed by thoroughly rinsing with distilled water at room temperature. After drying at 60℃, the silk protein was dissolved in 9.3 M LiBr solution at 60℃ for 4 h, and the solution was dialyzed with a dialyzed membrane (3500 molecular weight cutoff) against deionized water for 72 h at room temperature. Then the solution was enriched by PEG20000, and centrifuged at 9000 rpm twice at 4℃ for 20 min to remove aggregates. The SF solution with the final concentration of 6.0% (w/w) was obtained and stored at 4℃ before use.

2.2 Synthesis of NYp. NYp was synthesised by following typical solid phase synthesis procedures using Fmoc-L-Tyr(H_2PO_3)-OH, Fmoc-L-Phe-OH, Fmoc-Gly-OH, and 2-naphthylacetic acid. Briefly, 0.5g 2-chlorotrityl chloride resin was swelled in dry dichloromethane (DCM) with nitrogen (N_2) bubbling for 30 min and then was washed by dry dimethylformamide (DMF) five times. Afterward, the solution containing Fmoc-L-Tyr(H_2PO_3)-OH and *N,N*-diisopropylethylamine (DIEA) in DMF was added. After reaction for 1.5 h, the resin was rinsed by dry DMF four times and quenched by the blocking solution (80:15:5 of DCM/methanol/DIEA) for 10 min twice. Then, the resin was treated with 20% piperidine in DMF for 30 min and washed thoroughly with DMF 4 times. The peptide chain was prolonged by following standard Fmoc solid phase synthesis protocols with the application of HBTU as a coupling reagent. Finally, the synthesis peptide was cleaved from the resin by 95% trifluoroacetic acid and was purified by HPLC (eluents: H_2O:CH_3CN from 80:20 to 20:80). The final yield of NYp was ≈ 40%. ^{1}H NMR (400 MHz，DMSO-d_6)：δ (ppm) = 8.29-8.26 (d, 1H), 8.24-8.2 (t, 1H), 8.17-8.14 (d, 1H), 8.035-8.0 (d, 1H), 7.875-7.85 (d, 1H), 7.84-7.8 (t, 2H), 7.755-7.738 (s, 1H), 7.5-7.44 (m, 2H), 7.43-7.4 (d, 1H), 7.25-7.12 (m, 12H), 7.1-7.06 (d, 2H), 4.585-4.535 (m, 1H), 4.515-4.465 (m, 1H), 4.46-4.41 (m, 1H), 3.735-3.685 (m, 1H), 3.63-3.61 (s, 2H), 3.6-3.55 (m, 1H), 3.055-3.0 (m, 2H), 2.96-2.89 (m, 2H), 2.81-2.755 (m, 1H), 2.685-2.63 (m, 1H). MS: calcd M =780.77, obsd $[M+Na]^+$= 803.328, obsd $[M+K]^+$= 819.307.

2.3 Gelation tests of SF triggered by NYp and ALP. To investigate the abilities of NYp to trigger the gelation of SF, we prepared the stock solution of NYp with concentration at 0.5 wt% and pH=7.4. The varied concentrations of SF solutions (0.1%, 0.5%, 1.0%, and 2.0%) were prepared by diluting stock solution (6.0%) with deionized water. After adding designed volumes of NYp and to SF solution, followed by adding the ALP, we obtained the SF-NY hydrogels containing varied concentrations of NY (0.08, 0.1, 0.2 and 0.3 wt%), SF (0.1, 0.5, 1.0 and 2.0%) and ALP (10, 20 and 40 U/mL). Their gelation states were determined by tube-inversion methods.

2.4 In vitro release of ALP From the SF-NY gel. The SF-NY gel encapsulated 10 U/mL ALP was incubated in 2 mL PBS buffer. The concentrations of active ALP released from the hydrogel were determined by using a standard ALP activity assay at different times (1, 2, 4, 8, 16, 32, 48, 72, 96 and 120 h). Briefly, 200 μL PBS buffer containing released ALP was taken out, followed by the supplement of the same volume of PBS buffer. 100 μL of a substrate solution comprising 5×10^{-3} M p-nitrophenylphosphate disodiumsalt in 0.5 M alkaline buffer was added. After incubation in 3 min, 0.3 M NaOH solution was added to stop the reaction. Absorbance was measured at 405 nm. A calibration curve of ALP in PBS with concentrations ranging from 0 to 12.5 U/mL served as a reference.

2.5 Mineralization of the SF-NY gels. The SF-NY gels (SF=2.0%, NY=0.3 wt%, ALP=10 U/mL) were mineralized by incubation in different mineralized solution including (a) $CaCl_2$=10 mM, β-GP=6 mM; (b) $CaCl_2$=20 mM, β-GP=12 mM; and (c) $CaCl_2$=50 mM, β-GP=30 mM for 7 days with daily medium change at room temperature, which were named as the Ca-10, Ca-20 and Ca-50 gel, respectively. In addition, the SF-NY gels (SF=2.0%, NY=0.3 wt%) mineralized at different concentrations of ALP were conducted in the solution containing 20 mM of $CaCl_2$ and 12 mM of β-GP for 7 days with daily medium change at room temperature.

2.6 TEM, SEM and EDS Characterization. 10 μL of the sample was loaded onto a carbon-coated Cu grid, followed by staining with phosphotungstic acid (2.0%) for 10 min, and characterized by TEM (Hitachi HT7700, 120 kV). For SEM and EDS characterizations, the lyophilized gels were cut into thin slices, following by coating

with a thin layer of gold before SEM measurement. SEM and EDS were performed using Hitachi S-4700 microscope.

2.7 Circular Dichroism and FTIR Characterization. 20 μL of the sample was loaded into a 1 mm quartz cuvette and analysed by JASCO J-810 spectrometer under a nitrogen atmosphere from 180 nm to 400 nm. For FTIR characterization, the solutions and hydrogels were prepared by using deuterium oxid (D_2O) as a solvent, and DCl and NaOD as an acid and a base, respectively. FTIR spectra were collected on a Thermo Scientific Nicolet 6700 spectrophotometer with KBr cuvettes.

2.8 Rheological Measurement. 300 μL of the hydrogel was placed on a parallel plate of 20 mm diameter, and its rheological properties were examined on a Thermo Scientific HAAKE RheoStress 6000 rheometer at 25℃. (Ⅰ) The dynamic strain sweep tests were conducted from 0.01% to 100% strain at a fixed angular frequency of 1.0 Hz. (Ⅱ) The dynamic frequency sweep tests were measured from 0.1 to 100 Hz with strain at 1.0%. (Ⅲ) Alternate-step strain sweep tests were switched from a small strain (γ=1.0%) to a large strain (γ=100%) with 100 s for every strain interval at a fixed angular frequency (1 Hz).

2.9 XRD and XPS Characterization. The lyophilized gels were loaded onto coverslip and analysed by X'Pert-Pro MPD diffractometer (Panalytical, Netherlands) with CuKα radiation, with a wavelength of 1.54056 Å. The X-ray source was operated at 40 kV and 40 mA. The scanning speed was 5°/min with a step size of 0.026° and the 2θ range from 5° to 65°. Chemical analysis of the lyophilized samples was carried out on the X-ray photoelectron spectroscopy (XPS, Escalab 250XI, Thermo Fisher Scientific) by using Mg Kα line (1253.6 eV) with a passing energy of 11 eV.

2.10 In vitro cell biocompatibility measurements. The cytocompatibility of Ca-20 gel toward rBMSCs was assessed by live/dead assays. Primary rBMSCs were extracted according to previously reported procedures. The isolated rBMSCs were cultured in Dulbecco's Modified Eagle Medium (DMEM, Gibco, USA) containing 10% fetal bovine serum (FBS, Gibco, USA) and 1% penicillin-streptomycin (PS, Gibco, USA) at

37℃ and 5% CO_2. Before the cell culture, the Ca-20 gel was immersed in DMEM with 10% FBS for 30 min in the incubator. rBMSCs at a density of 1.5×10^4 cells/cm^2 were seeded on the surface of Ca-20 gel in 8-well borosilicate glass confocal plate and the medium was changed every other day. At the designed time points (1, 4 and 7 days), the cells were stained by calcein-AM/propidium iodide and visualized by a fluorescence microscopy (Zeiss, Axio, Germany). The cell densities were calculated by Image J software. Cells cultured on SF-NY gels and the bare wells of 8-well borosilicate glass confocal plates acted as controls. The cell counting kit-8 (CCK-8) assays were used to further measure cell viability and proliferation. Specifically, 300 μL of Ca-20 gel was coated on a 12-well plate, and then 1 ml of DMEM added onto the surface of the gels. After culturing 1, 4 and 7 days, 1 ml of fresh DMEM containing 10% CCK-8 solution (Dojindo Laboratories, Japan) were added to each well. After incubating for 2 h, 100 μL of the mixed medium was transferred to a 96-well plate. The optical density (OD) value of each sample was measured at 450 nm using a microplate reader (Infinite F50, Tecan, Switzerland). All experiments were performed in triplicate.

2.11 Alizarin Red S staining. To study osteogenic differentiation of rBMSCs on the scaffolds, Alizarin Red S staining was used to highlight mineralization nodules when the cells cultured on the Ca-20 gel for different days. 300 μL of Ca-20 gel was placed on a 12-well plate, and then rBMSCs were planted on the surface of gels at a density of 1×10^5 cells per well in standard growth medium (DMEM with 10% FBS). After 24 hours culturing, the culture medium was changed with osteoblastic induction medium (OIC) containing standard growth medium supplemented with 10^{-8} M dexamethasone, 50 μg/mL ascorbic acid, and 10 mM β-glycerophosphate (Sigma-Aldrich, USA) among all groups. At days 4, 7 and 14, the cells were washed with PBS for three times, and then fixed with 4% paraformaldehyde solution for 15 min. The fixed cells were further washed with distillated water for three times and then stained with 0.2% Alizarin Red S (Sigma-Aldrich, USA) solution for 10 min at 37℃. After washing three times with distillated water, the samples were air-dried and the stained cells were imaged under

microscopy. To quantify the orange-red coloration of Alizarin Red S, 1 ml 10% acetic acid was added to the cells for overnight incubation, and then the cells with the acetic acid were transferred to tubes and centrifuged for 20 min at 20,000 g. The supernatant was removed to other tubes and then neutralized with 10% ammonium hydroxide. 100 μL of each sample was transferred to a 96-well plate and the optical absorbance was measured at 405 nm with a microplate reader. Cells cultured on SF-NY gels and the bare wells of 12-well plates under the same conditions acted as controls. All tests were performed in triplicate.

2.12 Quantitative real-time PCR analysis. Quantitative real-time PCR (qRT-PCR) were used to further study osteogenic differentiation of rBMSCs on the Ca-20 gel by assessing the expression of osteogenesis-related genes, such as runt-related transcription factor 2 (Runx2), collagen type I (Col1α), osteocalcin (OCN), osteopontin (OPN). 300 μL of Ca-20 gel was placed on a 12-well plate, and then immersed in fresh DMEM for 30 min. After the medium removed, the cells were seeded on the surface of Ca-20 gel with a density of 1×10^5 cells per well in standard growth medium. After culturing for 24 hours, the culture medium was changed with osteoinductive medium. At different time points (4, 7 and 14 days), total RNA was extracted using a TRIzol reagent kit (Invitrogen, USA). Then 1 μg of total RNA was reverse transcribed to get complementary DNA by using PrimeScript RT reagent Kit (TakaRa, Japan) following the manufacture's protocol. Then, qRT-PCR was conducted using a SYBR Green qRT-PCR kit (TakaRa, Japan) and an ABI Step One Plus Real-Time PCR System (Applied Biosystems, US). The experimental data were processed by the $2^{-\Delta\Delta Ct}$ method. GAPDH was used as a reference and each sample was performed in triplicate. All primers are listed in Table 2. Cells cultured on SF-NY gels and the bare wells of 12-well plates under the same conditions acted as controls.

2.13 Rat femur defect model. The rat femur defect models were performed to study the osteogenic capacity of the Ca-20 gels in vivo. All experimental procedures involving rats were performed in compliance with the regulations for animal experiments of the Animal Ethics Committee of Shanghai Ruijin Hospital, and the Animal Ethics Committee of Shanghai Ruijin Hospital has approved the experiments. The animals had free access to both sterile water and standard rodent chow. All

experimental animals were used 10-week-old male Sprague Dawley (SD) rats and had an average weight of 320~350 g. Briefly, SD rats were anesthetized with an intraperitoneal injection of 2.5% pentobarbital sodium (40 mg kg^{-1} body weight). A bicortical channel was widened gradually to a diameter of 2.5 mm using a slow-speed electric drill irrigated by ice saline solution to avoid thermal necrosis. The surgical area was rinsed with saline solution and then 100 μL of Ca-20 gel was implanted into the defect. After implantation, the skin was sutured. SF-NY gel groups and the blank groups under the same conditions acted as controls.

2.14 Bone Micro-CT. The experimental rats were sacrificed by CO_2 asphyxiation at 4 or 8 weeks following surgical implantation. Femurs were harvested and then were fixed in 10% formalin. The morphology of the reconstructed femur was evaluated using a high-resolution micro-CT (Scanco Medical, Switzerland). The scanning parameters were as follows: resolution 20 μm, voltage 70 kV, current 130 μA, and filtration 0.5 mm aluminum. The obtained data were analysed using Scanco software. The Bone mineral density (BMD), bone tissue volume/total tissue volume (BV/TV), trabecular thickness (Tb.Th) and trabecular separation/spacing (Tb.Sp) were determined. All tests were performed in triplicate.

2.15 Histological and immunohistochemical analysis. After surgery at 8 weeks, femoral samples were harvested and were fixed in 4% paraformaldehyde for 48 h, decalcified in 10% EDTA for 8 weeks, and subsequently embedded in paraffin and sectioned. The 5 μm thick sections of samples were used for histological and immunohistochemistry analysis. Hematoxylin and eosin (H&E) staining and Masson's trichrome staining were applied for histological analysis. For immunohistochemical staining, slices were first dewaxed and hydrated utilizing EDTA solutions and blocked with serum for 30 min. Then the slices were incubated with antibodies including anti-OPN (Cell Signaling Technology, USA), anti-OCN (Abcam, USA), or anti-Col 1α (Abcam, USA) at 4 °C overnight. Then the slices were washed with PBS and incubated with appropriate secondary antibodies for 1 hour at 37 °C. After rinsing with PBS, diamidino-phenyl-indole (DAPI) was applied to stain the nuclei. Images were photographed by microscopy (Zessis, Germany). And signal intensities were quantified using Image J software.

2.16 Statistical Analysis. All obtained data were presented as mean ± standard deviations. Statistical analysis was conducted using GraphPad Prism V.6.00 Software

(USA). $p < 0.05$ was considered significant, unless otherwise indicated. One-way ANOVA with Tukey's multiple comparison was used to conduct statistic analysis.

3. Solid phase peptide synthesis of NYp

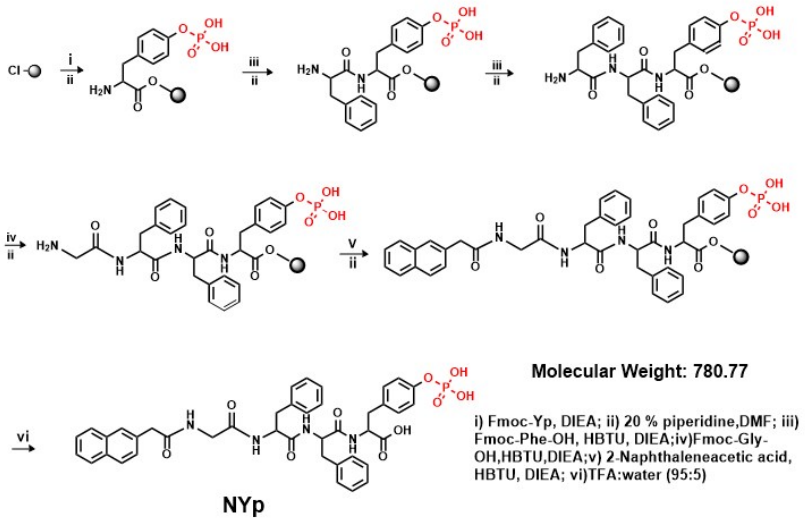

Fig. S1 Synthetic routes for the preparation of NYp via solid phase peptide synthesis.

4. ^{1}H and ^{31}P NMR of NYp

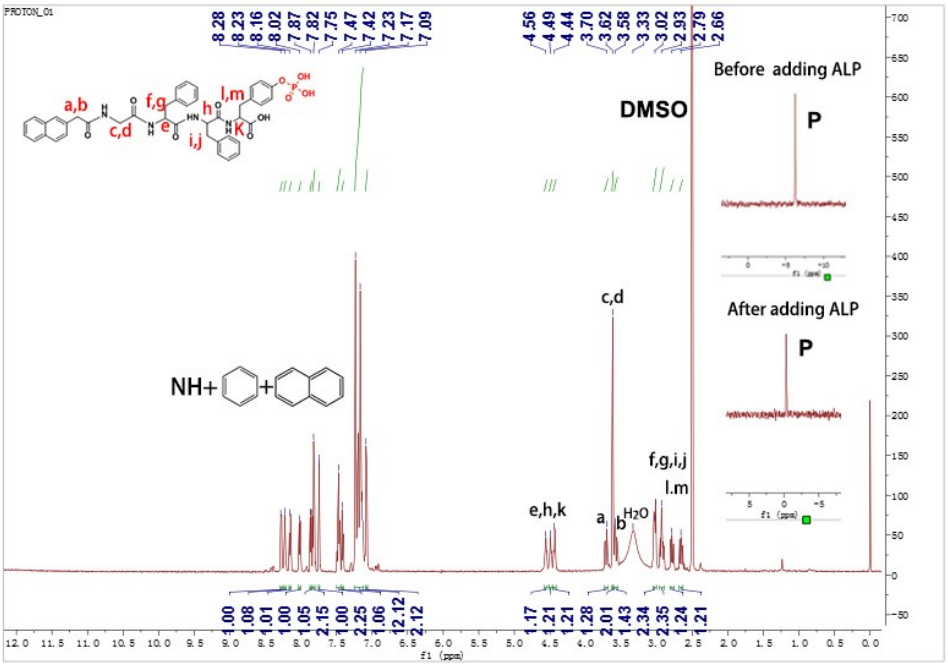

Fig. S2 ^{1}H and ^{31}P NMR of the NYp in DMSO-*d6*.

5. TOF-MS of NYp

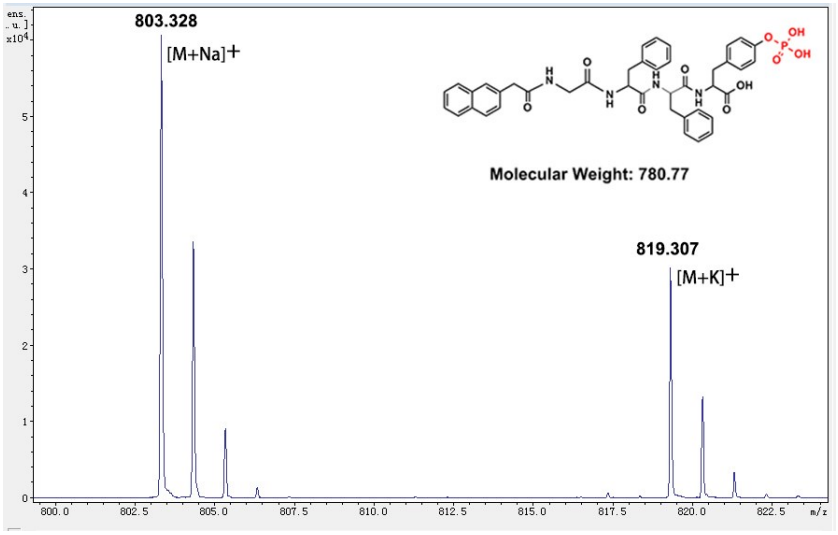

Fig. S3 MALDI-TOF MS of NYp.

6. Gelation test of the NY gel

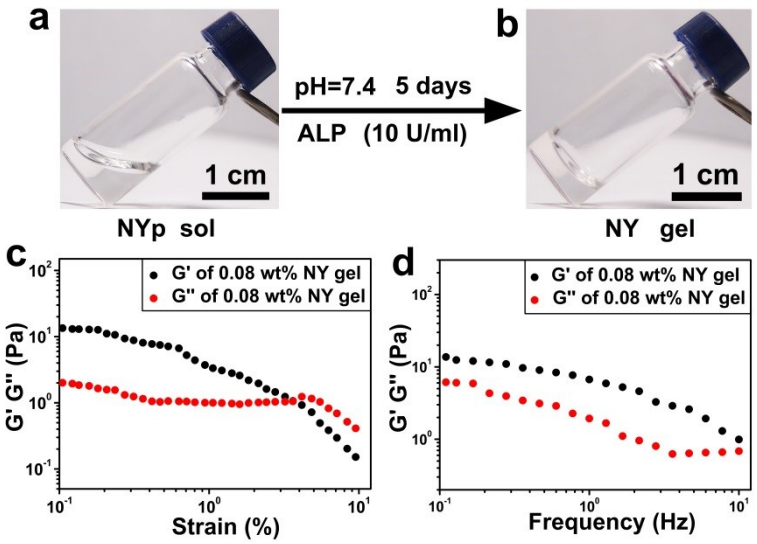

Fig. S4 Optical images of **(a)** the solution of NYp and **(b)** its self-assembled hydrogel at 0.08 wt% and pH=7.4 over 5 days. **(c)** Strain dependence and **(d)** frequency dependence of the dynamic storage modulus (G') and the loss modulus (G'') of the self-assembled NY gel (0.08 wt%, pH=7.4).

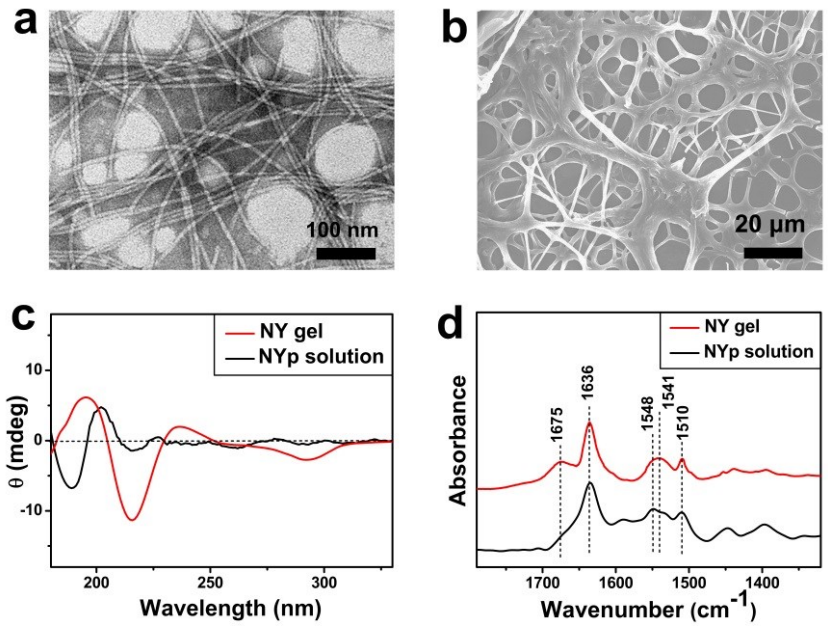

Fig. S5 (a) TEM and **(b)** SEM images of the self-assembled structures within the NY gel (0.3 wt%, pH=7.4). **(c)** CD and **(d)** FTIR spectra of the NYp solution (0.3 wt%) and the self-assembled NY gel (0.3 wt%, pH=7.4).

7. Gelation test of the SF gel

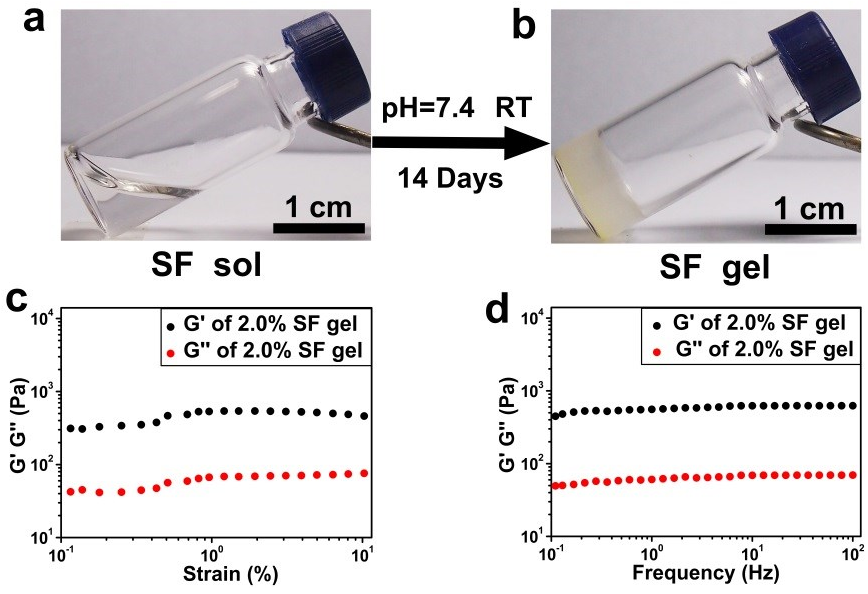

Fig. S6 Optical images of **(a)** the solution of SF and **(b)** its self-assembled hydrogel at 2.0% and pH=7.4 over 14 days. **(c)** Strain dependence and **(d)** frequency dependence of the dynamic storage modulus (G') and the loss modulus (G'') of the self-assembled SF gel (2.0%, pH=7.4).

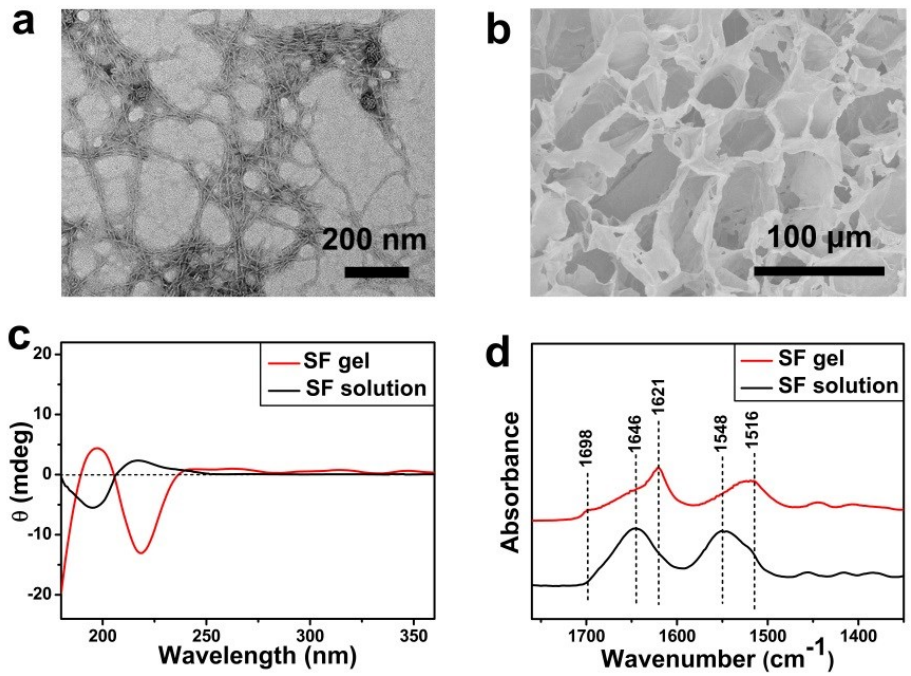

Fig. S7 (a) TEM and **(b)** SEM images of the self-assembled structures within the SF gel (2.0%, pH=7.4) shown in Figure S6b. **(c)** CD and **(d)** FTIR spectra of the SF solution (2.0%) and the self-assembled SF gel (2.0%, pH=7.4) shown in Figure S6b.

8. The gelation test of the NYp solution and SF solution without the presence of ALP

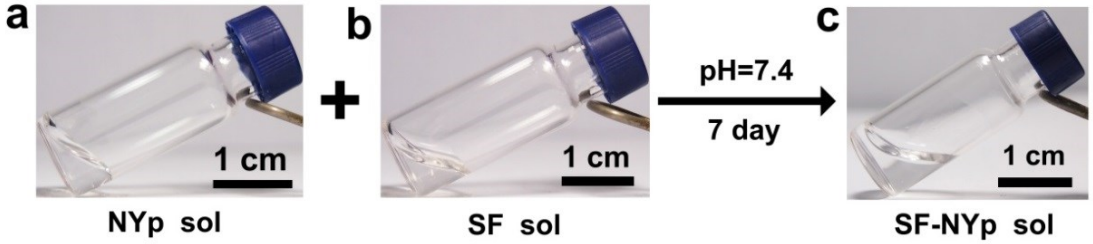

Fig. S8 Optical images of **(a)** the NYp solution (0.16 wt%, pH=7.4), **(b)** the blank SF solution (0.2%, pH=7.4), and **(c)** the SF-NYp solution (NYp=0.08 wt%, SF=0.1%, pH=7.4).

9. Gelation tests and rheological measurements of the SF-NY gel

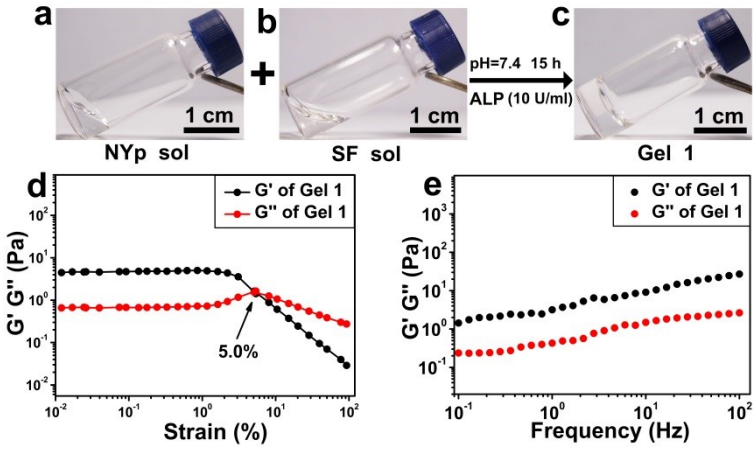

Fig. S9 Optical images of **(a)** the NYp solution (0.16 wt%, pH=7.4), **(b)** the blank SF solution (0.2%, pH=7.4), and **(c)** the SF-NY gel (NY=0.08 wt%, SF=0.1%, ALP=10 U/mL, pH=7.4). **(d)** Strain dependence and **(e)** frequency dependence of the dynamic storage modulus (G') and the loss modulus (G'') of the self-assembled SF-NY gel shown in Figure S9c.

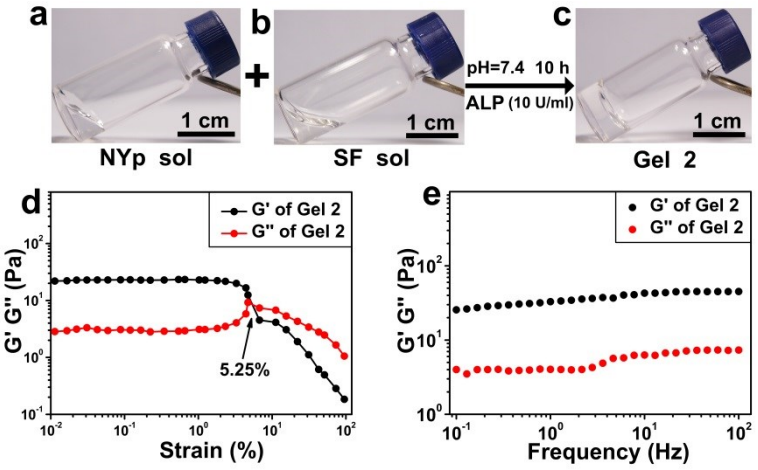

Fig. S10 Optical images of **(a)** the NYp solution (0.2 wt%, pH=7.4), **(b)** the blank SF solution (0.2%, pH=7.4), and **(c)** the SF-NY gel (NY=0.1 wt%, SF=0.1%, ALP=10 U/mL, pH=7.4). **(d)** Strain dependence and **(e)** frequency dependence of the dynamic storage modulus (G') and the loss modulus (G'') of the self-assembled SF-NY gel shown in Figure S10c.

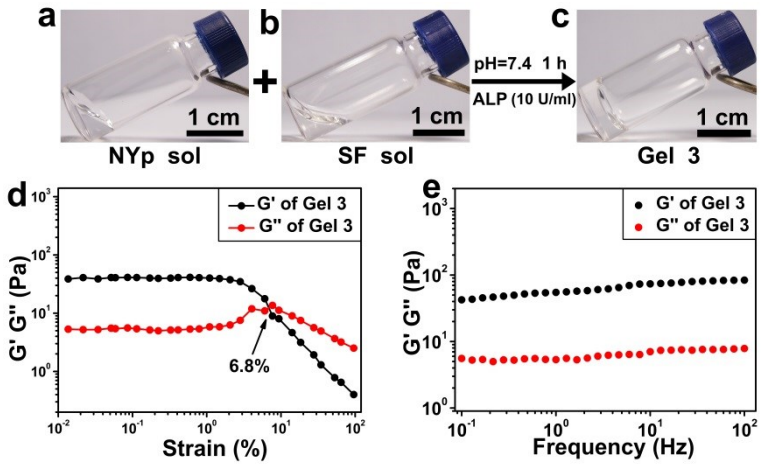

Fig. S11 Optical images of **(a)** the NYp solution (0.4 wt%, pH=7.4), **(b)** the blank SF solution (0.2%, pH=7.4), and **(c)** the SF-NY gel (NY=0.2 wt%, SF=0.1%, ALP=10 U/mL, pH=7.4). **(d)** Strain dependence and **(e)** frequency dependence of the dynamic storage modulus (G') and the loss modulus (G'') of the self-assembled SF-NY gel shown in Figure S11c.

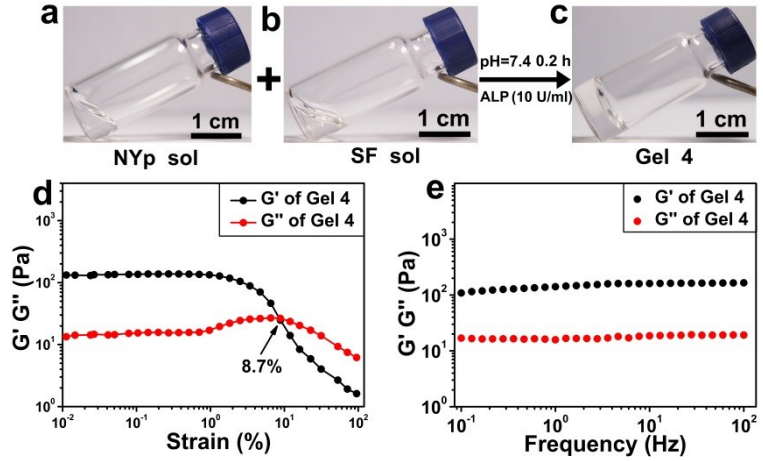

Fig. S12 Optical images of **(a)** the NYp solution (0.6 wt%, pH=7.4), **(b)** the blank SF solution (0.2%, pH=7.4), and **(c)** the SF-NY gel (NY=0.3 wt%, SF=0.1%, ALP=10 U/mL, pH=7.4). **(d)** Strain dependence and **(e)** frequency dependence of the dynamic storage modulus (G') and the loss modulus (G'') of the self-assembled SF-NY gel shown in Figure S12c.

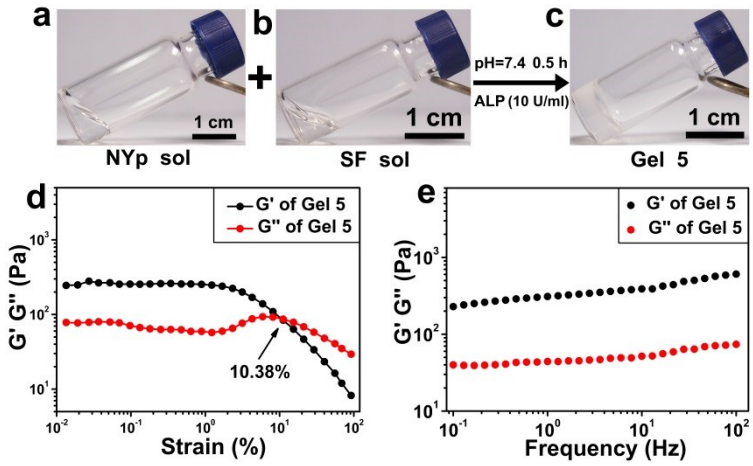

Fig. S13 Optical images of **(a)** the NYp solution (0.6 wt%, pH=7.4), **(b)** the blank SF solution (1.0%, pH=7.4), and **(c)** the SF-NY gel (NY=0.3 wt%, SF=0.5%, ALP=10 U/mL, pH=7.4). **(d)** Strain dependence and **(e)** frequency dependence of the dynamic storage modulus (G') and the loss modulus (G'') of the self-assembled SF-NY gel shown in Figure S13c.

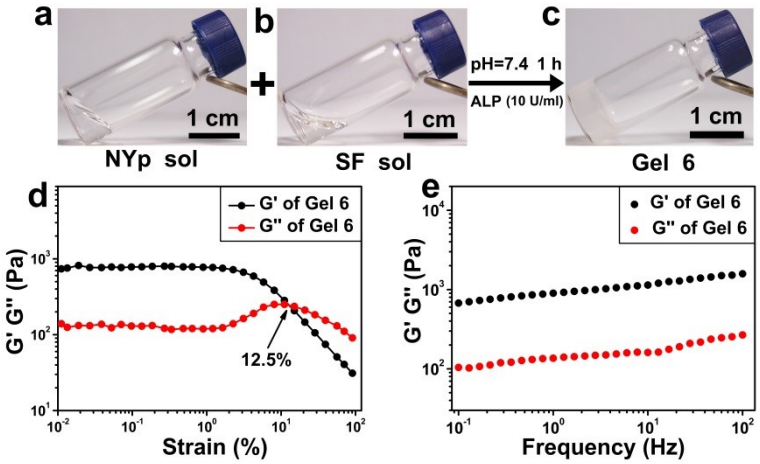

Fig. S14 Optical images of **(a)** the NYp solution (0.6 wt%, pH=7.4), **(b)** the blank SF solution (2.0%, pH=7.4), and **(c)** the SF-NY gel (NY=0.3 wt%, SF=1.0%, ALP=10 U/mL, pH=7.4). **(d)** Strain dependence and **(e)** frequency dependence of the dynamic storage modulus (G') and the loss modulus (G'') of the self-assembled SF-NY gel shown in Figure S14c.

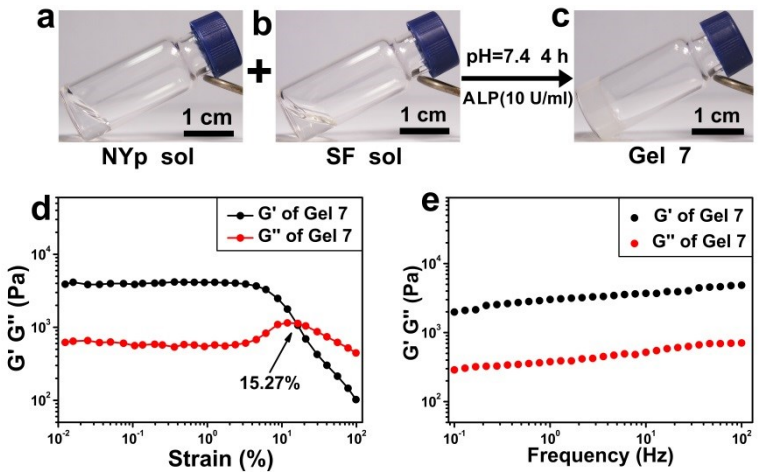

Fig. S15 Optical images of **(a)** the NYp solution (0.6 wt%, pH=7.4), **(b)** the blank SF solution (4.0%, pH=7.4), and **(c)** the SF-NY gel (NY=0.3 wt%, SF=2.0%, ALP=10 U/mL, pH=7.4). **(d)** Strain dependence and **(e)** frequency dependence of the dynamic storage modulus (G') and the loss modulus (G'') of the self-assembled SF-NY gel shown in Figure S15c.

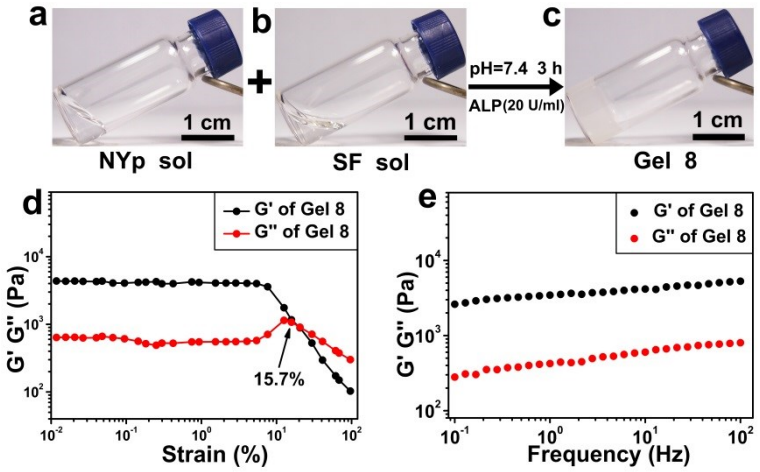

Fig. S16 Optical images of **(a)** the NYp solution (0.6 wt%, pH=7.4), **(b)** the blank SF solution (4.0%, pH=7.4), and **(c)** the SF-NY gel (NY=0.3 wt%, SF=2.0%, ALP=20 U/mL, pH=7.4). **(d)** Strain dependence and **(e)** frequency dependence of the dynamic storage modulus (G') and the loss modulus (G'') of the self-assembled SF-NY gel shown in Figure S16c.

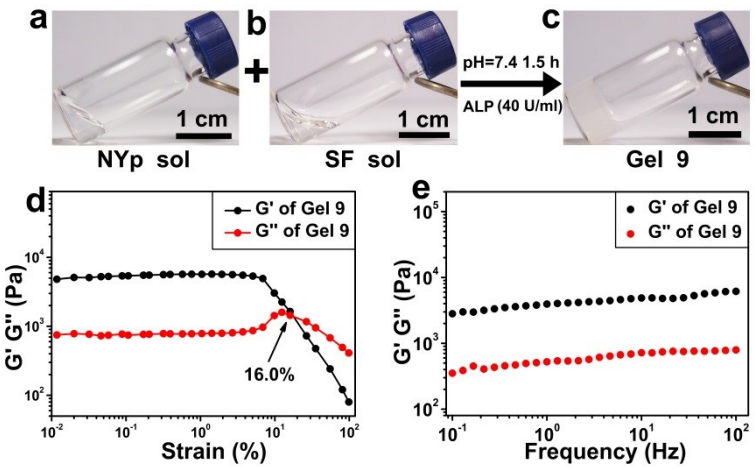

Fig. S17 Optical images of **(a)** the NYp solution (0.6 wt%, pH=7.4), **(b)** the blank SF solution (4.0%, pH=7.4), and **(c)** the SF-NY gel (NY=0.3 wt%, SF=2.0%, ALP=40 U/mL, pH=7.4). **(d)** Strain dependence and **(e)** frequency dependence of the dynamic storage modulus (G') and the loss modulus (G'') of the self-assembled SF-NY gel shown in Figure S17c.

Table S1. Summary of the conditions and properties of SF-NY gels

Sample	Sol	Gel 1	Gel 2	Gel 3	Gel 4	Gel 5	Gel 6	Gel 7	Gel 8	Gel 9
NYp (wt%)	0.05	0.08	0.1	0.2	0.3	0.3	0.3	0.3	0.3	0.3
SF (%)	0.1	0.1	0.1	0.1	0.1	0.5	1.0	2.0	2.0	2.0
pH	7.4	7.4	7.4	7.4	7.4	7.4	7.4	7.4	7.4	7.4
ALP (U/ml)	10	10	10	10	10	10	10	10	20	40
Optical images										
Gelation time	--	15 h	10 h	1 h	0.2 h	0.5 h	1 h	4 h	3 h	1.5 h
G' (Pa)	-- [a]	27	37	83	165	607	1582	4865	5289	6147

[a] The gelation process did not occur in 48 h.

10. SEM images of SF-NY gels prepared at different concentrations of SF and NY

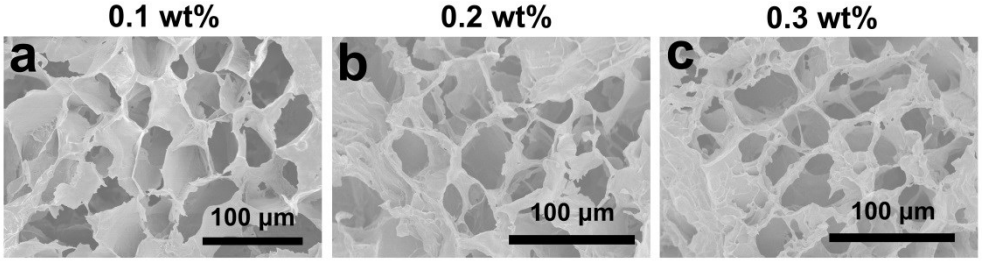

Fig. S18 SEM images of SF-NY gels containing 2.0% SF and different concentrations

of NY.

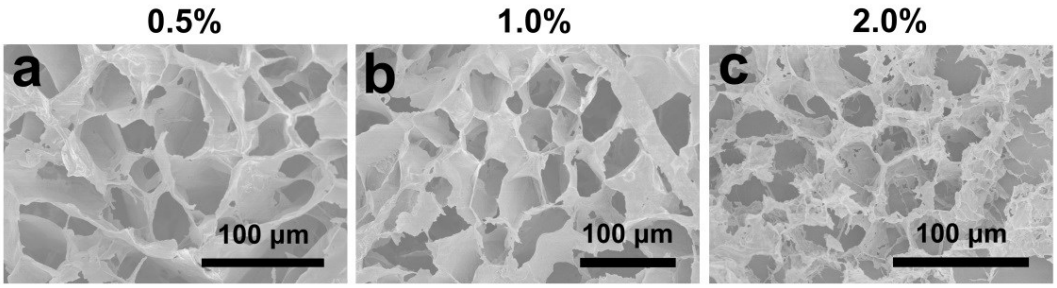

Fig. S19 SEM images of SF-NY gels containing 0.3 wt% NY and different concentrations of SF.

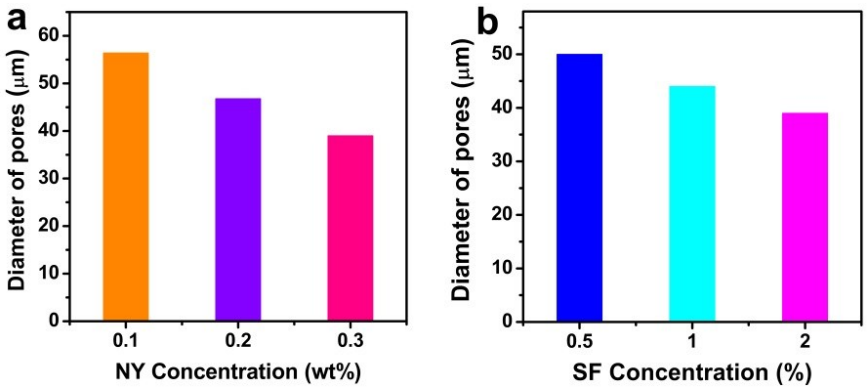

Fig. S20 (a) The sizes of porous structures within SF-NY hydrogels containing 2.0% SF and different concentrations of NY (0.1, 0.2 and 0.3 wt%). **(b)** The sizes of porous structures within SF-NY hydrogels containing 0.3 wt% NY and different concentrations of SF (0.5, 1.0 and 2.0%).

11. Determination of the binding constant between SF and NY

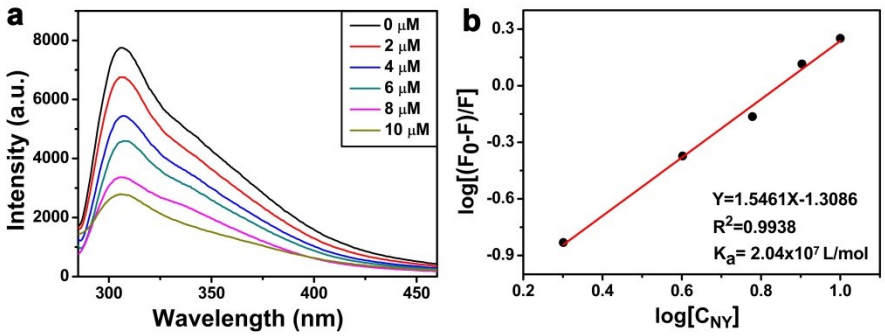

Fig. S21 (a) Fluorescence emission spectra of SF (2.0%) titrated with varying concentrations of NY in 10 mM PBS buffer (pH=7.4). **(b)** Double log Stern–Volmer plot of $(F_0\text{-}F)/F$ versus NY concentrations $[C_{NY}]$ to determine the binding constant

between NY and SF.

12. Rheological tests of the SF-NY gels at different concentrations of SF and ALP

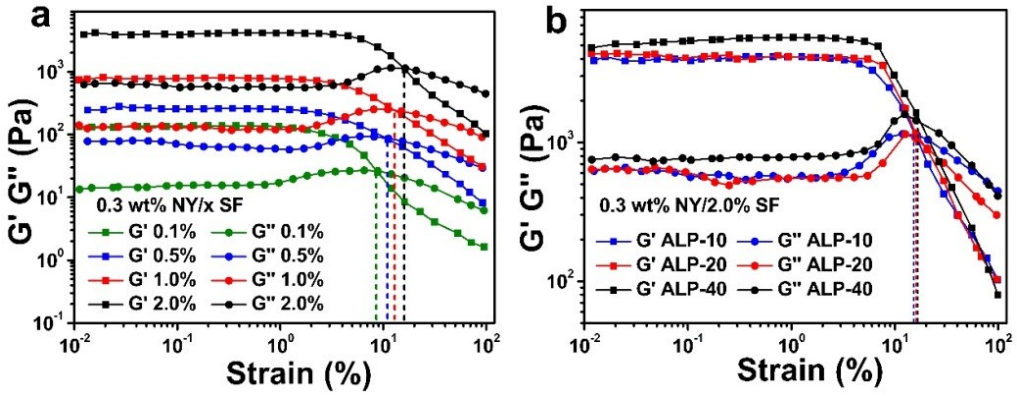

Fig. S22 Strain dependence of the dynamic storage modulus (G') and the loss modulus (G'') of various SF-NY gels at a fixed angular frequency (1 Hz). **(a)** NY=0.3 wt%, SF=0.1, 0.5, 1.0 and 2.0%, ALP=10 U/mL; **(b)** NY=0.3 wt%, SF=2.0%, ALP=10, 20 and 40 U/mL.

13. ALP release from the SF-NY gel in vitro

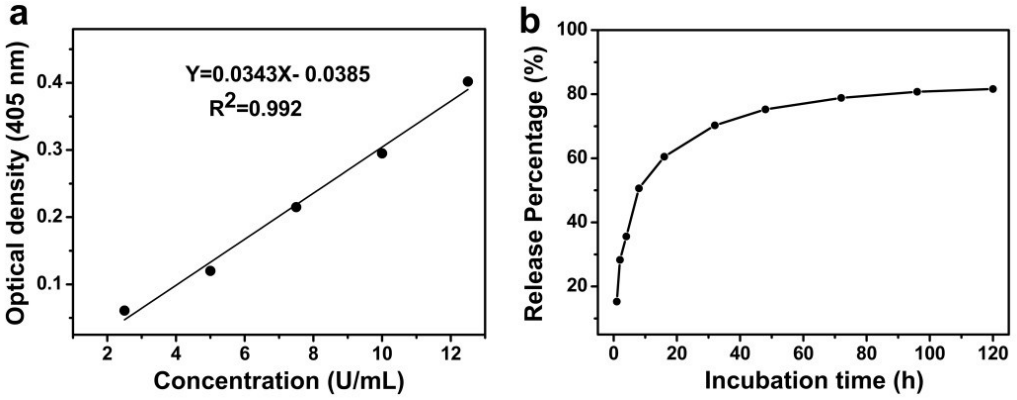

Fig. S23 (a) The calibration curve between the optical absorptions of ALP at 405 nm and ALP concentrations in solutions. **(b)** Cumulative release of ALP from the SF-NY gel (SF=2.0%, NY=0.3 wt%, ALP=10 U/mL) in PBS buffer.

14. SEM images of the Ca-20 gels prepared at different concentrations of ALP

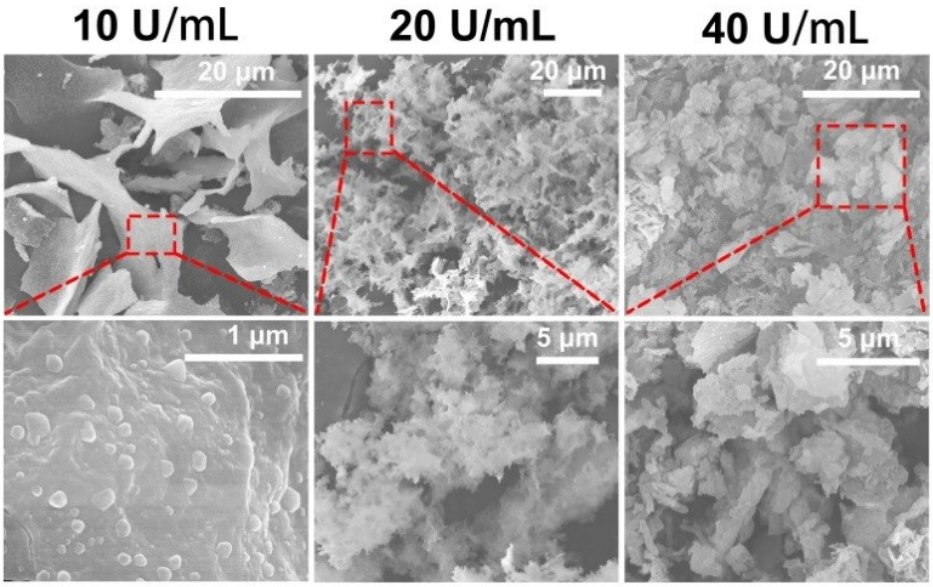

Fig. S24 SEM images of the Ca-20 gels prepared at different concentrations of ALP (10, 20 and 40 U/mL) after 7 day mineralization.

15. Rheological tests of the mineralized hydrogels prepared at different concentrations of Ca^{2+}

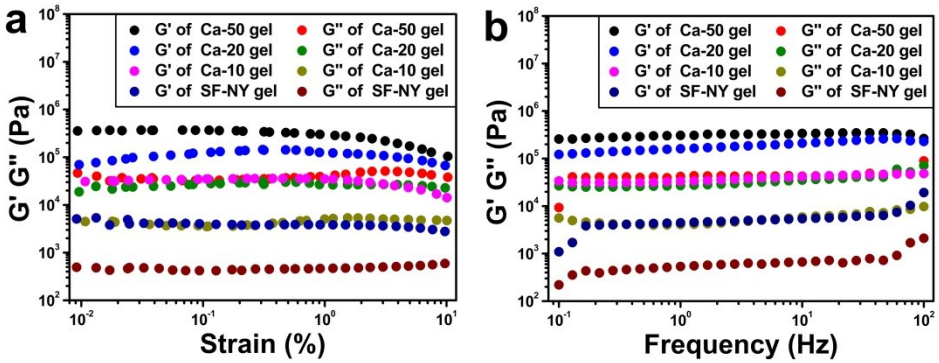

Fig. S25 (a) Strain dependence (0.01-10%) and **(b)** frequency dependence (0.1-100 Hz) of the dynamic storage modulus (G') and the loss modulus (G'') of the SF-NY gel (SF=2.0%, NY=0.3 wt%, ALP=10 U/mL) and the mineralized hydrogels containing varied concentrations of Ca^{2+} (SF=2.0%, NY=0.3 wt%, ALP=10 U/mL, Ca^{2+}=10, 20, 50 mM).

16. Stability test of the SF-NY gel and the Ca-20 gel in cell culture medium

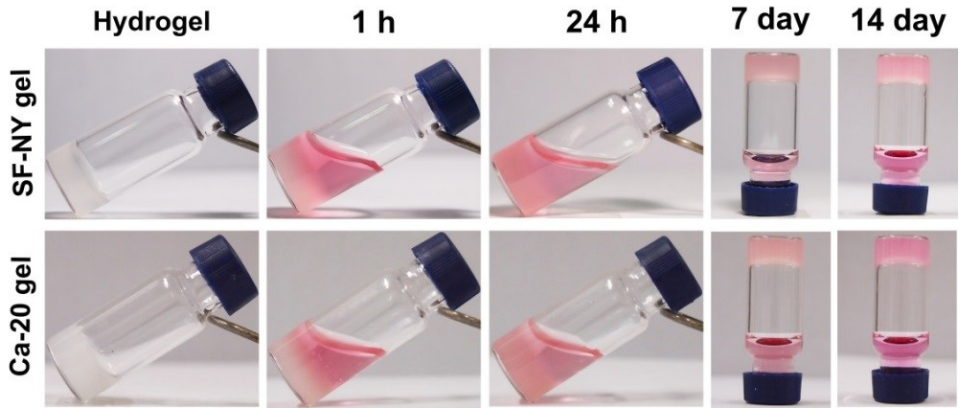

Fig. S26 The stability of the SF-NY gel (SF=2.0%, NY=0.3 wt %, ALP=10 U/mL) and the Ca-20 gel (SF=2.0%, NY=0.3 wt%, ALP=10 U/mL, Ca^{2+}=20 mM) in cell culture media at 37°C over the course of 14 days.

17. Table S2. Primers for Real-Time PCR Analysis

Gene	Forward Premier	Reverse Premier
OCN	5'-TGCTCACTCTGCTGACCCTG-3'	5'-TTATTGCCCTCCTGCTTG-3'
Runx-2	5'-GTGTCACTGCGCTGAAGAGG-3'	5'-GACCAACCGAGTCATTTAAGGC-3'
OPN	5'-GCCGAGGTGATAGTGTGGTT-3'	5'-TGAGGTGATGTCCTCGTCTG-3'
Col1a	5'-GAGGGCCAAGACGAAGACATC-3'	5'-CAGATCACGTCATCGCACAAC-3'
GAPDH	5'-ACAACTTTGGTATCGTGGAAGG-3'	5'-GCCATCACGCCACAGTTTC-3'